УДК 546.82-034.24:576.343:544.032.65
https://doi.org/10.20538/1682-0363-2026-2-101-114

Metabolic Reaction of Cells to Changes in the Physical and Chemical State of the Nitinol Surface Induced by Ultraviolet Laser Radiation with a Wavelength of 266 nm

Khlusov I.A.[1, 2], Kokorev O.V.[1], Gorokhova A.V.[1, 2], Nasibov T.F.[1, 2], Krivoshchekov S.V.[1], Chebodaeva V.V. [2, 3], Brazovsky K.S.[1], Khlusova M.Yu.[1], Sablina T.Yu.[2], Kandaurova M.Yu.[2], Zyatikov I.A.[2], Panchenko Yu.N.[2]

[1] *Siberian State Medical University*
2 Moskovsky trakt, 634050 Tomsk, Russian Federation

[2] *Institute of High Current Electronics, Siberian Branch of the Russian Academy of Sciences (IHCE SB RAS)*
2/3 Akademichesky Ave., 634055 Tomsk, Russian Federation

[3] *Institute of Strength Physics and Materials Science, Siberian Branch of the Russian Academy of Sciences (ISPMS SB RAS)*
2/4 Akademichesky Ave., 634055 Tomsk, Russian Federation

ABSTRACT

Aim. MTT (methylthiazolyldiphenyl-tetrazolium bromide) viability assessment of the *in vitro* cellular response to changes in the physicochemical properties (zeta potential, wettability, topography) of the nitinol surface after treatment with ultraviolet (UV) laser radiation (UV-LR) with a wavelength of 266 nm.

Materials and methods. The MCF-7 cell culture was incubated with nitinol-based alloy plates for 24 hours, before and after exposure to UV light (wavelength 266 nm, energy density 0.1 J/cm²) with a Q-smart 850 pulsed Nd:YAG laser. The samples were then analyzed for roughness (*Ra*) (GOST 2789-73) and surface contact angle with water. Zeta (ζ) potentials were also measured for both nitinol-based alloy substrates (SurPASS 3) and MCF-7 cells (Litesizer DLS 500). Metabolic activity of the cells was assessed using the MTT test, as recommended by GOST ISO 10993-5-2023 for the *in vitro* assessment of the cytotoxicity of medical materials and devices. Bioinformatics *in silico* analysis of intracellular signaling and metabolic pathways was conducted using the WikiPathways database.

Results. Surface modification caused by UV-LR significantly reduced the toxic response (decrease in metabolic activity) of MCF-7 cells to the nitinol-based alloy substrate. UV-LR did not affect the zeta potential (±10 mV from the isoelectric point), but it significantly decreased the water contact angle (from 75 to 8.7°) and increased the *Ra* index of surface roughness (from 71.5 nm to 93.9 nm). *In silico* mechanotransduction analysis revealed that the roughness and hydrophilicity/hydrophobicity of nitinol can independently induce gene expression in MCF-7 cells, as well as through cross-talking molecular mechanisms. At the same time, several signaling pathways (WP5504, WP3680, WP5477, WP3941, WP5046, and WP2435) were found to be close to those involved in the reduction of the MTT reagent, which is used as a marker for the cell death program induced by metabolic imbalance in MCF-7 cells.

Conclusion. UV-LR promotes an increase in hydrophilicity and/or nanoroughness of the nitinol-based alloy surface, but it does not affect the zeta potential. This may initiate a cascade of molecular mechanisms regulating cellular and tissue responses to implanted materials. These events can include inflammation, hemostasis activation, angiospasm, vessel regeneration, and metabolic activity of target cells.

Keywords: MCF-7 cells, MTT test, *in vitro*, stent substrates, zeta-potential, wettability, roughness, *in silico* modeling

✉ *Khlusov Igor A.,* khlusov63@mail.ru

Conflict of interest. The authors declare the absence of obvious or potential conflict of interest related to the publication of this article.

Source of financing. The study was carried out with support from the Russian Science Foundation grant No. №25-79-31008.

For citation: Khlusov I.A., Kokorev O.V., Gorokhova A.V., Nasibov T.F., Krivoshchekov S.V., Chebodaeva V.V., Brazovsky K.S., Khlusova M.Yu., Sablina T.Yu., Kandaurova M.Yu., Zyatikov I.A., Panchenko Yu.N. Metabolic Reaction of Cells to Changes in the Physical and Chemical State of the Nitinol Surface Induced by Ultraviolet Laser Radiation with a Wavelength of 266 nm. *Bulletin of Siberian Medicine.* 2026;25(2):101–114. https://doi.org/10.20538/1682-0363-2026-2-101-114.

Метаболическая реакция клеток на изменение физико-химического состояния поверхности никелида титана, индуцированное ультрафиолетовым лазерным излучением с длиной волны 266 нм

Хлусов И.А.[1, 2], Кокорев О.В.[1], Горохова А.В.[1, 2], Насибов Т.Ф.[1, 2], Кривощеков С.В.[1], Чебодаева В.В.[2, 3], Бразовский К.С.[1], Хлусова М.Ю.[1], Саблина Т.Ю.[2], Кандаурова М.Ю.[2], Зятиков И.А.[2], Панченко Ю.Н.[2]

[1] *Сибирский государственный медицинский университет (СибГМУ)*
Россия, 634050, г. Томск, Московский тракт, 2

[2] *Институт сильноточной электроники Сибирского отделения Российской академии наук (ИСО СО РАН)*
Россия, 634055, г. Томск, пр. Академический, 2/3

[3] *Институт физики прочности и материаловедения Сибирского отделения Российской академии наук (ИФПМ СО РАН)*
Россия, 634055, г. Томск, пр. Академический, 2/4

РЕЗЮМЕ

Цель: оценка с помощью 3-[4,5-диметилтиазол-2-ил]-2,5-дифенилтетразолия бромида (MTT) клеточной реакции *in vitro* на изменение физико-химического состояния (дзета-потенциала, смачиваемости, топографии) поверхности сплава на основе никелида титана (нитинола) после обработки ультрафиолетовым лазерным излучением (УФ-ЛИ) с длиной волны 266 нм.

Материалы и методы. Клеточную культуру MCF-7 инкубировали в течение 24 ч с пластинами из сплава на основе никелида титана, до и после обработки УФ-ЛИ (плотность энергии 0,1 Дж/см^2). На образцах измеряли индекс шероховатости *Ra* (ГОСТ 2789-73) и контактный угол смачивания поверхности водой. Дзета-потенциалы поверхности подложек из нитинола и MCF-7 клеток определяли с использованием анализаторов для плоских образцов (SurPASS 3) и частиц (Litesizer DLS 500) соответственно. Метаболическую активность клеточной культуры определяли с помощью MTT-теста, рекомендуемого ГОСТ ISO 10993-5-2023 для оценки *in vitro* цитотоксичности медицинских материалов и изделий. Биоинформатический *in silico* анализ внутриклеточных сигнальных и метаболических путей осуществляли в базе данных WikiPathways.

Результаты. Модификация поверхности УФ-ЛИ статистически значимо снижала токсический отклик (падение метаболической активности) MCF-7 клеток на контакт с подложкой из нитинола. Обработка УФ-ЛИ не влияла на величину дзета-потенциала, но существенно уменьшала контактный угол смачивания водой (с 75 до 8,7°), а также повышала *Ra* поверхности образцов (с 71,5 до 93,9 нм). Анализ *in silico* с позиций механотрансдукции показал, что шероховатость и гидрофильность (гидрофобность) нитинола могут индуцировать экспрессию генов в MCF-7 клетках независимо друг от друга, а также через перекрестные молекулярные механизмы. При этом некоторые сигнальные пути (WP5504, WP3680, WP5477, WP3941, WP5046, WP2435) близки к системам, участвующим в редукции MTT-реагента как маркера программы клеточной смерти, индуцированной метаболическим дисбалансом MCF-7 клеток.

Заключение. Обработка УФ-ЛИ способствует увеличению гидрофильности и (или) наношероховатости, но не дзета-потенциала поверхности подложек из нитинола. Это может инициировать каскад молекулярных механизмов, регулирующих клеточно-тканевые реакции на имплантируемые материалы, включая индукцию воспаления, активацию гемостаза, ангиоспазм и регенерацию кровеносного русла, а также метаболическую активность клеток-мишеней.

Ключевые слова: MCF-7 клетки, МТТ-тест, *in vitro*, подложки для стентов, дзета-потенциал, смачиваемость, шероховатость, *in silico* моделирование

Конфликт интересов. Авторы декларируют отсутствие явных и потенциальных конфликтов интересов, связанных с публикацией настоящей статьи.

Источники финансирования. Исследование выполнено при поддержке гранта Российского научного фонда № 25-79-31008.

Для цитирования: Хлусов И.А., Кокорев О.В., Горохова А.В., Насибов Т.Ф., Кривощеков С.В., Чебодаева В.В., Бразовский К.С., Хлусова М.Ю., Саблина Т.Ю., Кандаурова М.Ю., Зятиков И.А., Панченко Ю.Н. Метаболическая реакция клеток на изменение физико-химического состояния поверхности никелида титана, индуцированное ультрафиолетовым лазерным излучением с длиной волны 266 нм. *Бюллетень сибирской медицины.* 2026;25(2):101–114. https://doi.org/10.20538/1682-0363-2026-2-101-114.

INTRODUCTION

Cardiovascular diseases are the leading cause of mortality worldwide [1]. The primary method of urgent minimally invasive therapy for coronary artery disease, one of the most common circulatory system pathologies, is stenting of arteries affected by atherosclerosis and arterial hypertension. Currently, there are more than 400 types of stents, differing in material composition, dimensions, design, coating for the blood-contacting surface, delivery system into the blood vessel, etc.

For some time, it was believed that the main challenges of stenting (thrombosis and arterial restenosis) would be solved by composite drug-eluting stents (DES). However, due to the high risk of late (occurring 6 months after implantation) thromboses associated with DES [2], preference is commonly given to metal stents, which hold a definitive clinical niche [3]. Nitinol alloy attracts the attention of researchers and clinicians due to its superelastic behavior, which allows implants to deform congruently with blood vessel walls over a long period, as well as to withstand the cyclic fatigue resistance threshold for cardiovascular devices, which is 15 million cycles in mechanical tests [4].

However, the high (up to 57 wt.%) concentration of nickel (Ni) in nitinol poses a threat of its release into the bloodstream and penetration into the vascular wall due to stent corrosion. Ni exhibits pronounced toxicity (Hazard Class 1–2; GOST 32419-2022), allergenicity, and carcinogenicity [5]. To improve the corrosion resistance of nitinol, various surface modification methods are being proposed, including those utilizing ion – plasma technologies [5] and concentrated energy flows (electron beam, laser radiation).

Recently, laser processing of nitinol-based alloys has attracted researchers' attention as a method that allows for the wide-ranging modification of the physicochemical properties of the surface layer without affecting the beneficial functional properties of the medical device [6, 7]. The team from the Gas Lasers Laboratory at ISE SB RAS is developing a laser surface modification method for nitinol using ultraviolet (UV) laser radiation ($\lambda < 400$ nm) [8, 9], which requires investigation of the biocompatibility of the modified devices.

In this regard, the aim of the study was to perform the MTT assessment of the *in vitro* cellular response to changes in the physical and chemical state (zeta (ζ) potential, wettability, topography) of the nitinol surface after treatment with UV laser radiation.

MATERIALS AND METHODS

Plates measuring 10 × 10 × 1 mm^3 (length × width × thickness) made of a nitinol-based alloy were used for the study. The material was developed at the Research Institute of Medical Materials and Shape Memory Implants (Tomsk, Russia). Pre-treatment of the sample surface (grinding, polishing, and ultrasonic cleaning), measurement of the contact wettability angle, and surface topography were performed as described in [8]. The average surface

roughness index *Ra* was measured in accordance with GOST 2789-73.

UV (wavelength 266 nm) laser modification of the nitinol sample surfaces was carried out using a Q-smart 850 pulsed Nd:YAG laser (Quantel, France) generating pulses with a duration of 5 ns and a frequency of 10 Hz (Fig.1). The laser beam diameter was d = 5 mm, the step between scanning lines was h_y = 0.25 cm, the energy density was j = 0.1 J/cm², and the scanning speed was V_x = 375 μm/s.

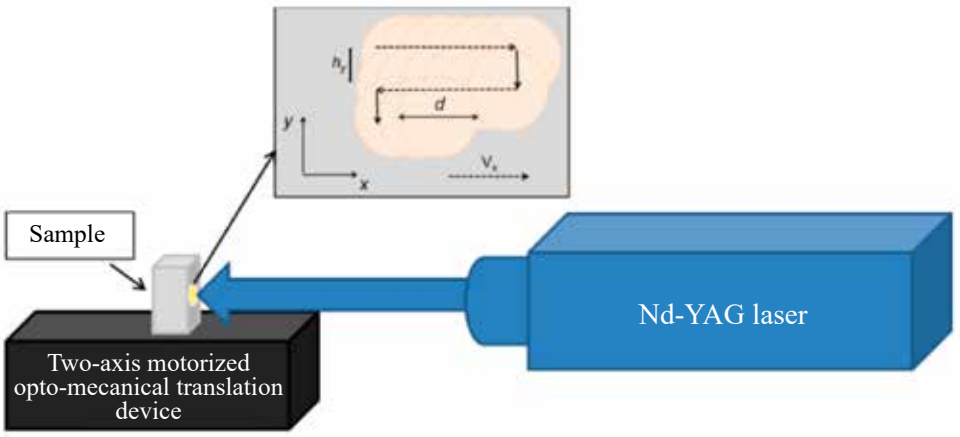

Fig. 1. Schematic diagram of the UV-laser surface processing of samples and the laser scanning principle

The ζ-potential of the nitinol sample surfaces before and after UV laser treatment was determined using a SurPASS 3 electrokinetic analyzer for flat samples (Anton Paar GmbH, Austria) in accordance with the manufacturer's instructions. The samples were mounted pairwise (opposite each other) in an adjustable gap cell with a gap width of up to 100 μm (98 μm in the current experiment). A 0.001 M KCl solution with pH ~7 was used as the background electrolyte. The pH of the electrolyte varied within the range of 3.0 – 8.5 units at a pressure of 200–600 mbar by adding 0.05 M KOH or HCl to the background electrolyte. The SurPASS 3 software calculated the ζ-potentials using the Helmholtz – Smoluchowski equation, as described previously [10].

The ζ-potential of MCF-7 cells was determined using a Litesizer DLS 500 particle analyzer (Anton Paar GmbH, Austria) with its integrated software in accordance with the manufacturer's instructions. A cell suspension at a concentration of 50×10^4 per 1 ml of the RPMI-1640 medium with low calcium content at pH = 7.0–7.2 was placed into the instrument measurement cell. The automated measurement cycle relative to a reference electrolyte (phosphate buffered saline) comprised 100–1,000 cells to achieve a normal distribution of the variable (Fig.2).

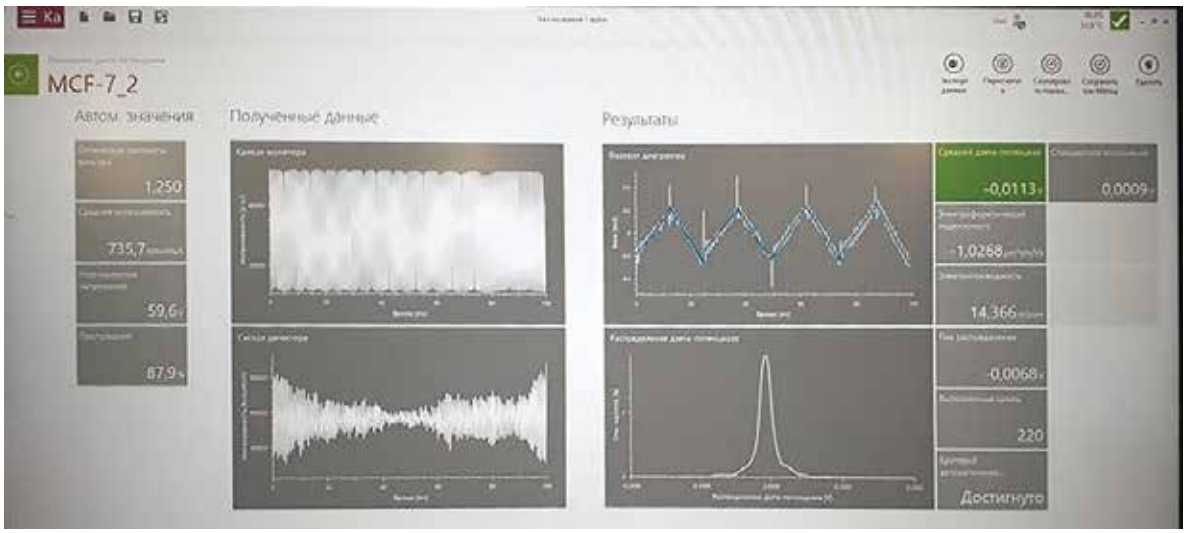

Fig. 2. Interface of the particle analyzer software during the measurement of the ζ-potential of MCF-7 cells

To determine the cellular response upon contact with the nitinol samples (plates measuring 10 × 10 × 1 mm^3), which were preliminarily sterilized by dry heat at 180 °C for 60 minutes, the MCF-7 cells of human invasive ductal adenocarcinoma (Institute of Cytology, Russian Academy of Sciences, St. Petersburg) were employed.

The cells were co-cultured with the test objects for 24 hours in 24-well flat-bottom plates (Orange Scientific, Braine-l'Alleud, Belgium) at a concentration of 50×10^4 viable cells per 1 ml of the nutrient medium with the following composition: 90% Dulbecco's Modified Eagle Medium (DMEM) (Servicebio, China), 10% fetal bovine serum (Technozero, Russia), antibiotics (100 units/ml penicillin and 100 μg/ml streptomycin, Capricon Scientific, Germany), and 2 mM L-glutamine (PanEco, Russia).

Four hours prior to the end of the cultivation period, the cell cultures were detached from the plastic surface of the culture plates. The *in vitro* cytotoxicity index (CI) for the control (cell culture without nitinol substrates) and the test group (cells + nitinol samples) was determined, as described in [11], using a 0.5% solution of 3-[4,5-dimethylthiazol-2-yl]-2,5-diphenyltetrazolium bromide (MTT) (NeoFroxx, Germany), as recommended by GOST ISO 10993-5-2023.

The bioinformatics *in silico* analysis of signaling and metabolic pathways, as well as associated genes potentially expressed in the MCF-7 cells in response to stimuli (keywords: "surface roughness", "surface wettability") was performed using the open-access GeneCards database (https://www.genecards.org/). Subsequently, an over-representation analysis (ORA) was conducted for each resulting gene list according to the algorithm described in [12, 13]. Common metabolic pathways relevant to the study focus were then identified.

Statistical data analysis was performed using the R programming language (version 4.5.1) with the MVN [14], PMCMRplus [15], and brunnermunzel [16] packages. The compliance of quantitative variables with a normal distribution was assessed using the Shapiro – Wilk test with the Royston's correction [17]. Quantitative, normally distributed variables were described as the mean and the standard deviation ($M \pm SD$). Quantitative variables that were not normally distributed and ordinal variables were described as the median and the interquartile range ($Me\ [Q_1; Q_3]$).

For comparing the means of two samples with a normal distribution, the Welch's *t*-test [21–23] was used as a more powerful test that does not require equality of variances, unlike the classical Student's *t*-test [18–20].

For comparing two independent samples that did not comply with a normal distribution, the Brunner – Munzel test [27, 28] was applied as a more robust and versatile method compared to the Mann – Whitney *U*-test, since it does not require assumptions about the equality of distributions and/or variances [29, 30].

For multiple comparisons of groups with a normal distribution but unequal variances, the Welch's analysis of variance (Welch's ANOVA) was employed, which does not require preliminary testing for homogeneity of variances [31, 32] and controls the type I error rate [32–35]. Subsequent pairwise comparisons were performed using the Games – Howell post-hoc test due to its robustness to violations of homoscedasticity and high statistical power [36, 37].

RESULTS

MCF-7 cells adhere to plastic, exhibit variable sizes (up to 50 μm), and display variable morphology (rounded or fibroblast-like) (Fig.3).

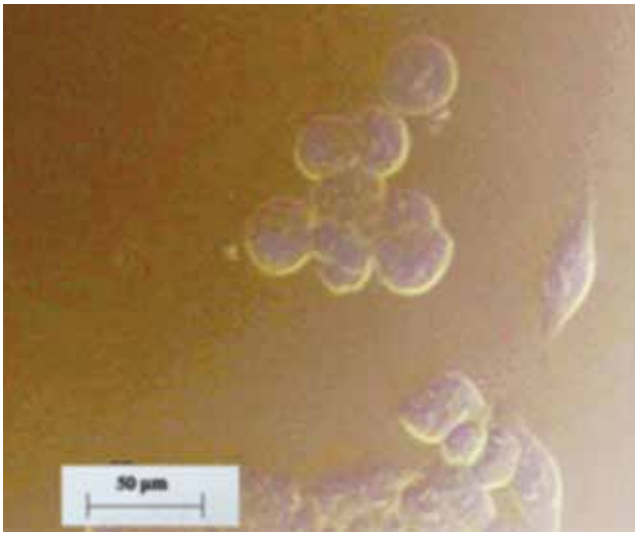

Fig. 3. Morphology of adherent MCF-7 cells after 24 hours of cultivation. Unstained native preparation, dark-field microscopy. Scale bar: 50 μm.

The MTT test showed (Fig.4) that during short-term *in vitro* contact of the cell suspension with the

studied nitinol substrates, which simulate the surface state of vascular stents, a decrease in the metabolic activity of the cells was observed. This was recorded by reduced (relative to the control culture) formation of the colored metabolite (formazan) from the MTT reagent. Such a result is interpreted as a marker of cell death at a median CI of 33%. This value slightly exceeds the threshold (30%) recommended by GOST ISO 10993-5-2023 as conditionally safe for determining the *in vitro* cytotoxicity of medical materials and devices. The physicochemical modification of the surface with UV laser radiation statistically significantly (Brunner – Munzel test, $p < 0.001$) reduced the toxic cell response upon contact with the test device to the 30% recommended by the regulatory document (Fig.4). This indicates less significant inhibition of the metabolic activity of the MCF-7 cells upon contact with the modified metal substrate.

From a fundamental perspective, the probable cause-and-effect relationships underlying this phenomenon are of interest.

To better understand the physicochemical changes in the surface state induced by UV laser radiation, the ζ-potential of the samples was investigated (Fig.5). The experimental electrokinetic curves (Fig.5, *a*) showed that across a wide pH range for both types of nitinol surface (initial and laser-treated), the measured potential amplitude varied mainly within ±10 mV from the isoelectric point. For the statistical assessment of the effect of laser surface modification, the pH range of 6–8 was selected for

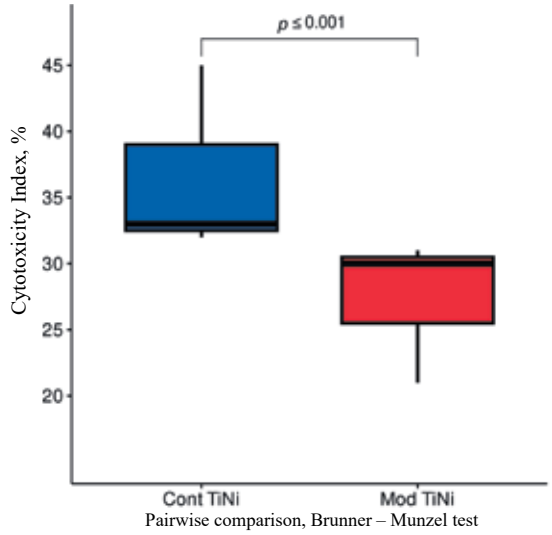

Fig.4. Results of the MTT test after 24-hour cultivation of the MCF-7 cells on unmodified (control, Cont nitinol) and modified (Mod nitinol) with UV laser radiation nitinol substrates. The X-axis, – group names; and the Y-axis – CI, %, *Me* [Q_1; Q_3] (pairwise comparison, Brunner – Munzel test, $p < 0.001$)

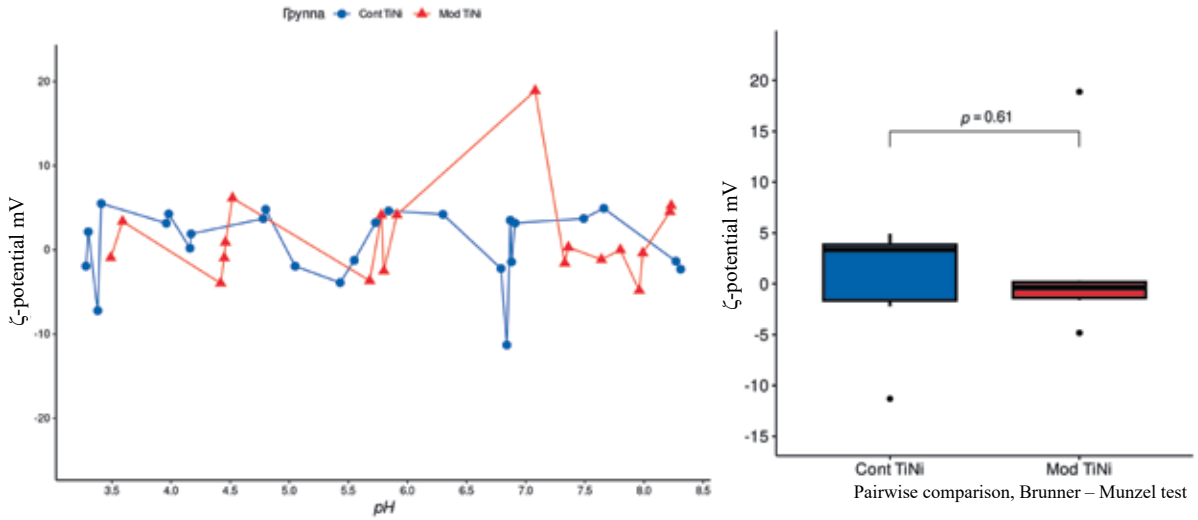

Fig. 5. Dependence of the amplitude and sign of the zeta potential on the tested nitinol samples on the pH of the solutions: *a* – pH = 3–8.5 (the X-axis – pH values, the Y-axis – ζ-potential, mV); *b* – pH = 6–8 (the X-axis – group names, the Y-axis – ζ-potential values, mV); *Me* [Q_1; Q_3], Brunner – Munzel test, $p = 0.61$

the following reasons: 1) in this region of electrolyte ionic strength, the maximum overshoots of the ζ-potentials with opposite charge signs occurred (Fig.5, *a*); 2) according to GOST R 52770-2016, the permissible change in the solvent pH after contact with the test device should not exceed ±1 unit from the physiological level of pH ~7–7.4.

The median values did not show a statistically significant effect of UV laser irradiation on the amplitude of the electrokinetic potential of the samples (Fig.5, *b*). In the meantime, the MCF-7 cells carried a negative surface charge with a potential amplitude of 11.3–11.6 mV (Fig.6).

Based on the obtained result, it was hypothesized that the change in the metabolic activity of the MCF-7 cells (Fig.4) was not associated with the ζ-potential of the modified nitinol surface under the selected mode of UV laser treatment. Nitinol in both study groups maintains an electrically neutral surface when exposed to a flow of the model electrolyte. The MTT molecule carries a positive charge [38] and can therefore penetrate the cytoplasmic membrane of MCF-7 cells, which carry a negative surface charge, via an electrostatic mechanism [39]. The identical charge and amplitude of the ζ-potential on the surface of both the initial and modified nitinol samples apparently do not affect the interaction between the reagent and the cell population.

Fig. 7 shows the result of the change in the contact wettability angle of the nitinol sample surfaces before and after UV-laser processing. Laser modification led to a drastic increase in the hydrophilicity of the samples; the contact angle decreased to 8.7°, which is 8.5 times smaller (Welch's *t*-test, $p < 0.001$) than the baseline value (Fig. 7). This corresponds to a superhydrophilic surface state, where the water contact angle approaches 0° [40].

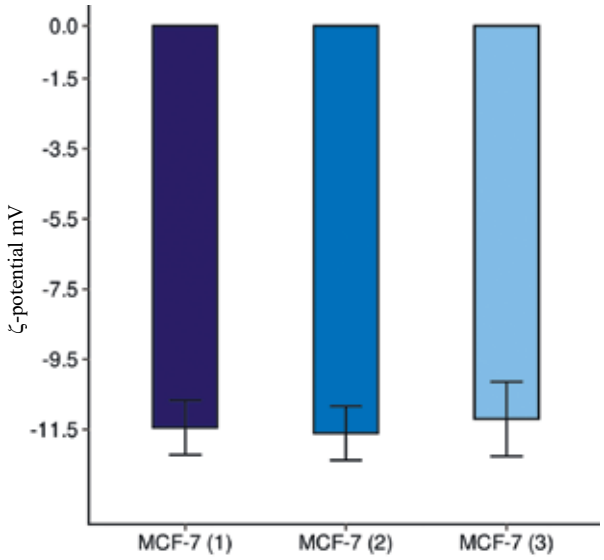

Fig. 6. Amplitude and sign of the zeta potential of the MCF-7 cells in the pH range of 6–8; the X-axis – cell line name and sample numbers, the Y-axis – ζ-potential values, mV; $M \pm SD$ (multiple comparison, one-way Welch's ANOVA, $p = 0.91$)

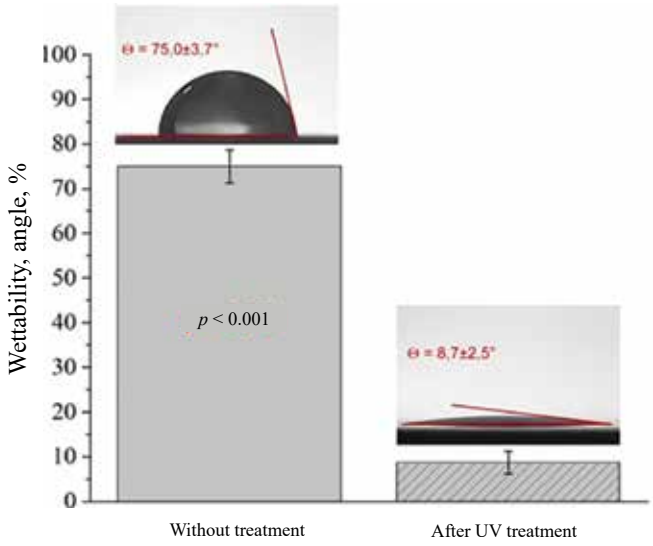

Fig. 7. Contact wettability angle and characteristic images of water droplets on the surface of nitinol samples before and after surface modification: the X-axis – group names, the Y-axis – wettability angle, °, $M \pm SD$ (5 measurements for each group, pairwise comparison, Welch's *t*-test, $p < 0.001$)

Surface wettability is influenced by its phase and elemental composition, as well as its topography (texture and roughness) [41–43]. The measured average roughness value *Ra* for the sample in its initial state was 71.5 ± 6.3 nm (class 11 of surface roughness according to GOST 2789-73) (Fig.8). After laser treatment (at an energy density of $j = 0.1$ J/cm^2), the surface profile did not change (Fig.8, *a*). However, it became more textured, and the average *Ra* value increased to 93.9 ± 9.6 nm (Welch's *t*-test, $p = 0.0041$), which corresponds to class 10 surface irregularity range (Fig.8, *b*).

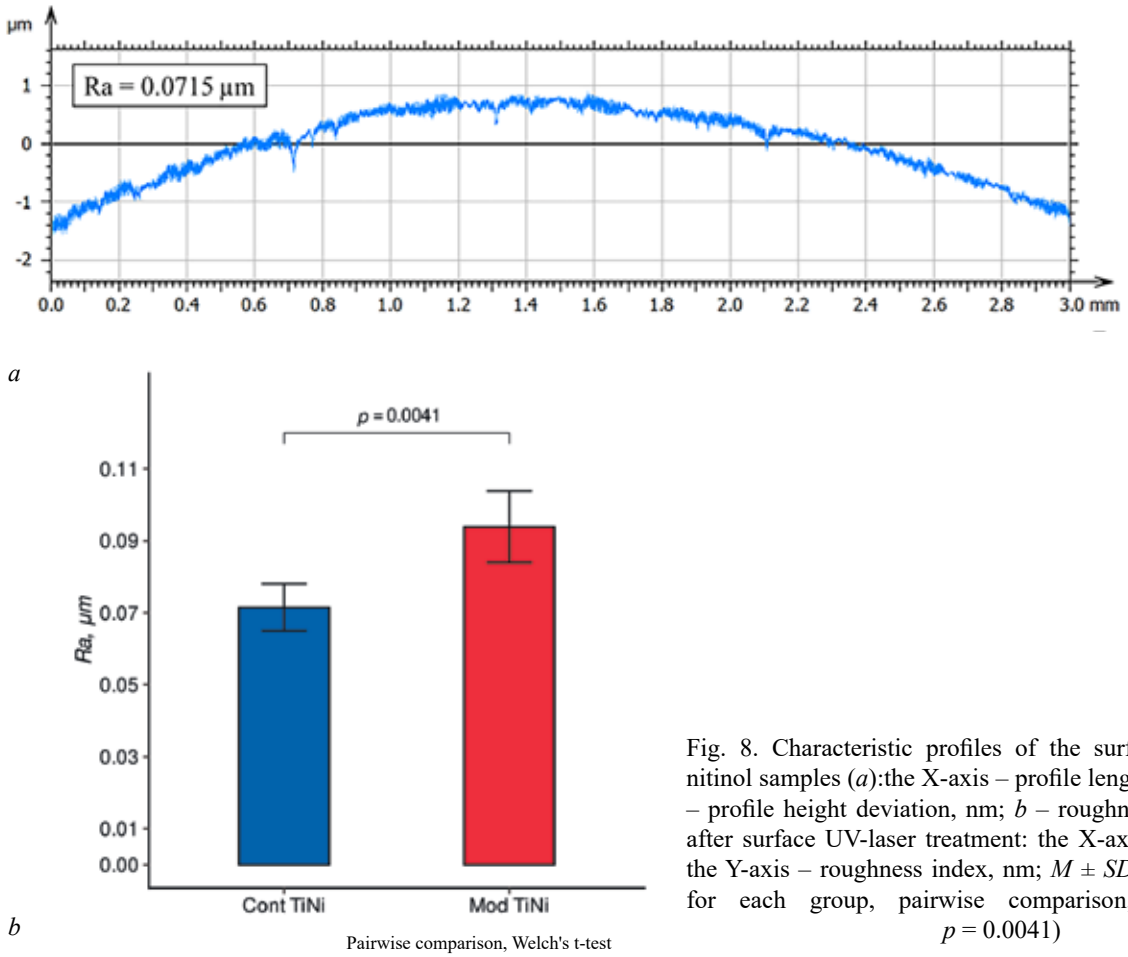

Fig. 8. Characteristic profiles of the surface of the tested nitinol samples (*a*):the X-axis – profile length, mm, the Y-axis – profile height deviation, nm; *b* – roughness *Ra* before and after surface UV-laser treatment: the X-axis – group names, the Y-axis – roughness index, nm; *M* ± *SD* (5 measurements for each group, pairwise comparison, Welch's *t*-test, $p = 0.0041$)

DISCUSSION

The MCF-7 cell line is widely used for determining the *in vitro* cytotoxicity of substances, scaffolds, and various medical materials and devices [11, 44–48], including stents for cardiovascular surgery [49]. Furthermore, the metabolism and signaling pathways of MCF-7 cells have been studied in considerable detail. For instance, a PubMed search for "MCF-7 cell metabolism" yielded 33,360 results, starting from the year 1975.

The MTT test is considered to be the gold standard for assessing cytotoxicity [50] based on the metabolic activity of the tested cells and is recommended by GOST ISO 10993-5-2023 for this purpose. The reduction of the MTT reagent into formazan granules is visualized in various cellular compartments (mitochondria, cytoplasm, nucleus, cytoplasmic membrane, microsomes) and is mediated by various enzymatic systems, including glycolysis and the mitochondrial respiratory chain [38].

A modern mechanotransduction theory postulates the translation of diverse stressors ((bio)physical and (bio)chemical forces (signals) from the macro- and microenvironments) into the cell nucleus via the cytoskeleton and intracellular signaling pathways [51–53]. Accordingly, diverse physicochemical signals from external stimuli are converted into variants of a cellular response through feedback mechanisms that regulate the expression of specific gene groups [53].

The intimate molecular (metabolic) processes underlying the functioning of the mechanotransduction system ("stressor – pathway – gene expression – cellular response") remain largely unelucidated. Nevertheless, certain properties of the natural and synthetic (scaffolds) extracellular matrix (ECM) that are capable of initiating signal transduction, thereby regulating cell behavior, are already known to varying degrees. These can be conditionally divided into (bio)physical (charge sign and ζ-potential amplitude, topography dimensionality), (bio)mechanical (elasticity/stiffness, compliance), and (bio)chemical (wettability (hydrophilicity or hydrophobicity), free energy, chemical composition,

solubility) stimuli [54–56], including in the context of the cardiovascular system [57–59].

For ECM and implants contacting blood, the sign of the surface charge and the amplitude of the electrostatic (in air) and electrokinetic potential are of great importance [60], since most cells in the body carry a negative surface charge [61], including blood cells [62], as well as the vascular endothelium [62, 63] and MSCs [64].

Thus, the ζ-potential value on human umbilical vein endothelial cells (HUVEC) is –17.1 ± 1.7 mV [65]. The amplitudes we measured for MCF-7 cells varied from –11.3 to –11.6 mV (Fig.6), which, according to the results of [65], is close to the values for another tumor cell line (–13.2 ± 1.2 mV, HeLa cells). In this regard, the MCF-7 cells of adenocarcinoma isolated from human breast ducts can be an adequate tool for modeling the interaction of cells with the surface of materials developed for cardiovascular stents.

Furthermore, such studies are beneficial because inflammation of the vascular wall, which inevitably occurs in the stent area [66], may promote the chemotaxis and tissue invasion of tumor cells circulating in the blood. Another possible scenario is the emigration of malignant cells from a tumor into the blood, induced by the implanted device. In this regard, studying the mechanisms of tumor cell adhesion to vascular implants is significant for the advancement of not only cardiovascular surgery but also oncology.

Artificial surfaces with ζ-potential fluctuations ranging from –10 mV to +10 mV are considered to be electrically neutral. According to [67], such materials will be bioinert towards circulating blood provided they possess high hydrophilicity. UV laser modification did not affect the neutral ζ-potential values (Fig.5).

Based on this fact, a hypothesis was put forward that the increased cell survival on nitinol after laser treatment (Fig.4) might be associated with the resulting superhydrophilic state of the modified surface (Fig.7). It is believed that mammalian cells prefer to adhere to hydrophilic substrates [68]. However, cells (for example, L-929 fibroblasts) can exhibit enhanced adhesion to both hydrophilic (after exposure to UV laser radiation) [69] and hydrophobic surfaces [70] of biomaterials.

The topography of the ECM undoubtedly influences the behavior of various cells (endothelial cells, smooth muscle cells, platelets) [71]. However, in each specific case, research results are ambiguous. On the one hand, MCF-7 cells adhere better and increase cell mass on rougher, bioinert gold electrode surfaces [72]. On the other hand, according to [73], an increase in the *Ra* value of the nano relief on a polymer surface (polyethylene terephthalate, PET) from 3.5 nm to 19 nm, conversely, stimulates apoptosis of MCF-7 cells. The surface chemistry and wettability of gold and PET differ significantly. Our results on nitinol suggest an improvement in the viability (metabolic activity) of MCF-7 cells on the rougher, hydrophilic surface induced by UV laser radiation (Fig.7, 8).

Next, a bioinformatics approach (Table) was used to predict potential intracellular mediators capable of transforming the action of physicochemical stimuli into gene expression and the corresponding cellular response. For MCF-7 cells, the ORA detected 358 target pathways for the query “surface roughness” and 39 for the keyword “surface wettability”, which does not seem surprising, given greater publication activity on the influence of topography on cell behavior.

We conditionally divided the found metabolic pathways into groups that may be relevant to the cellular and tissue reactions of the blood system to implantable materials (Table), including the induction of inflammation, activation of hemostasis, angiospasm and regeneration of the vascular bed, and metabolic activity. On one hand, the roughness and wettability of nitinol can induce a response in MCF-7 cells via their own signaling pathways. On the other hand, the search engine predicted several molecular mechanisms common to both stressors (WP453, WP5088, WP98, WP5036, and WP5158; Table), which can be interpreted as potential synergism or antagonism between roughness and wettability (hydrophilicity/hydrophobicity) regarding the ultimate response of MCF-7 cells.

Also of interest in Table is the group of pathways “Metabolic Activity and Cell Behavior”, where some entries (WP5504, WP3680, WP5477, WP3941, WP5046, WP2435) are related to the signaling and enzymatic intracellular systems involved in the reduction of the MTT reagent [39] as a marker of the cell death program [74] caused by a metabolic imbalance in MCF-7 cells.

In terms of discussion, it should be emphasized that both hydrophilicity and hydrophobicity are considered as beneficial biomedical/functional properties for medical devices contacting blood [75, 76].

Table

Target Intracellular Metabolic Pathways of MCF-7 Cells for Extracellular Matrix Mechanotransduction Factors (Roughness, Wettability) according to *in silico* Modeling Using the WikiPathways Database Search Engine

ID	Pathway name	Number of target genes	q-value < 0.05 for stressors		Common pathway for stressors
			Wettability	Roughness	
	Inflammation				
WP453	Inflammatory response	2/3	0.0033	0.0026	+
WP5088	Prostaglandin signaling	8	–	<0.001	
WP98	Prostaglandin synthesis and regulation	3	–	0.0072	+
WP4493	Cells and molecules involved in local acute inflammatory response	4	–	<0.001	–
WP5473	Cytokine receptor interaction	14	–	<0.001	–
WP530	Cytokines and inflammatory response	5	–	<0.001	–
WP75	Toll like receptor signaling	7	–	<0.001	–
WP4542	Leukocyte – intrinsic Hippo pathway functions	2	–	0.0334	–
	Hemostasis				
WP2806	Complement system	2	0.0135	–	–
WP272	Blood clotting cascade	1	0.018	–	–
WP558	Complement and coagulation cascades	1	0.0278	–	–
WP4462	Platelet mediated interactions with vascular and circulating cells	4	–	<0.001	–
	Circulatory system				
WP5036	Angiotensin II receptor type 1 pathway	1/2	0.0184	0.023	+
WP5158	Urotensin II mediated signaling	1/7	0.0278	<0.001	+
WP560	TGF beta receptor signaling	5	–	<0.001	–
WP3888	VEGFA VEGFR2 signaling	8	–	0.0155	–
WP4331	Neovascularization processes	2	–	0.0361	
	Metabolic activity and cell behavior (proliferation, differentiation, apoptosis)				
WP5156	Glyoxylate metabolism	1	0.0167	–	–
WP4172	PI3K Akt signaling	2	0.0206	–	–
WP5504	Disorders of mitochondrial homeostasis dynamics, protein import and quality control	1	0.0277	–	–
WP3680	Physicochemical features and toxicity-associated pathways	1	0.0278	–	–
WP4534	Mechanoregulation and pathology of YAP/TAZ via Hippo and non-Hippo mechanisms	4	–	<0.001	–
WP5477	Molecular pathway for oxidative stress	4	–	<0.001	–
WP3941	Oxidative damage response	3	–	0.0051	–
WP5046	NAD metabolism in oncogene-induced senescence and mitochondrial dysfunction-associated senescence	3	–	0.0012	–
WP2435	Quercetin and Nf kB AP 1- induced apoptosis	2	–	0.009	–
WP2911	miRNA targets in ECM and membrane receptors	2	–	0.0377	–

This is not surprising, since blood is a complex medium capable of wetting almost any artificial surface. Accordingly, *ex vivo* modification of the wettability of cardiovascular devices may not fulfill the useful practical role intended by materials scientists. At the same time, the technological minimization of surface topography is a more straightforward task in the manufacture of cardiovascular devices [77]. Consequently, it is necessary to determine a UV-laser treatment regimen that improves or does not affect the nanoscale roughness of stent substrates.

CONCLUSION

Metal stents, including those made of nitinol, are a modern tool of choice for cardiac surgeons in the minimally invasive treatment of arterial stenosis in various parts of the vascular bed. In turn, laser surface treatment can mitigate negative physicochemical properties (the corrosive activity of nitinol) and improve the bio- and hemocompatibility of cardiovascular devices. In this regard, UV laser modification of the nitinol surface (at an energy density of 0.1 J/cm^2) reduces the metabolic imbalance of cells adhering to the samples in an *in vitro* culture, which improves their survival rates according to the MTT test.

From the perspective of the experimental model and the bioinformatics prediction of the cause-and-effect relationships behind the obtained effect, the increased hydrophilicity and nanoscale roughness, but not the ζ-potential, of the nitinol substrates modified with UV laser radiation may underlie the induction of a cascade of intracellular signaling and metabolic pathways involved in the expression and transcription of genes regulating the cellular and tissue reactions of the blood system to implantable

materials. These reactions include the induction of inflammation, activation of hemostasis, angiospasm and regeneration of the vascular bed, as well as the metabolic activity of target cells. Further experimental verification of the actual expression of target genes and the response of target cells (endothelial cells, blood cells, mesenchymal stem cells, smooth muscle cells) to the physicochemical modification of the nitinol substrate surface is necessary.

REFERENCES

1. Usacheva E.V., Nelidova A.V., Kulikova O.M., Flyanku I.P. Mortality of Russian Able-bodied Population from Cardiovascular Diseases. *Hygiene and Sanitation*. 2021;100(2):159–165. (In Russ.). DOI: 10.47470/0016-9900-2021-100-2-159-165.
2. Camici G.G. What is an optimal stent? Biological requirements of drug eluting stents. *Kardiovaskuläre Medizin*. 2008;11(1):22–25.
3. Mani G., Feldman M.D., Patel D., Agrawal C.M. Coronary stents: a materials perspective. *Biomaterials*. 2007;28(9):1689–1710. DOI: 10.1016/j.biomaterials.2006.11.042.
4. U.S. Food and Drug Administration, Center for Devices and Radiological Health. Technical considerations for non-clinical assessment of medical devices containing Nitinol [draft guidance]. Silver Spring (MD): U.S. Food and Drug Administration; 2021 Jul 15 [updated 2021 Jul 15; cited 2024 Aug 10]. Available from: https://www.fda.gov/media/145294/download
5. Fukushima O., Yoneyama T., Doi H., Hanawa T. Corrosion resistance and surface characterization of electrolyzed Ti-Ni alloy. *Dental Materials Journal*. 2006;25(1):151–60. DOI: 10.4012/dmj.25.151.
6. Pequegnat A., Michael A., Wang J., Lian K., Zhou Y., Khan M.I. Surface characterizations of laser modified biomedical grade NiTi shape memory alloys. *Materials Science and Engineering: C*. 2015;50:367–378. DOI: 10.1016/j.msec.2015.01.085.
7. Chenrayan V., Vaishnav V., Shahapurkar K., Dhanabal P., Kalayarasan M., Raghunath S. et al. The effect of fs-laser micromachining parameters on surface roughness, bio-corrosion and biocompatibility of nitinol. *Optics & Laser Technology*. 2024;170:110200. DOI: 10.1016/j.optlastec.2023.110200.
8. Sablina T.Yu., Panchenko M.Yu., Zyatikov I.A., Puchikin A.V., Konovalov I.N., Panchenko Yu.N. Study of Surface Hydrophilicity of Metallic Materials Modified by Ultraviolet Laser Radiation. *Metal Working and Material Science*. 2024;26(4):218–233. (In Russ.). DOI: 10.17212/1994-6309-2024-26.4-218-233.
9. Panchenko M.Yu., Sablina T.Yu., Zyatikov I.A., Puchikin A.V., Panchenko Yu.N. Effect of UV laser treatment on wetting properties of TiNi alloy. *Russian Physics Journal*. 2024;67(10):1575–1582. DOI: 10.1007/s11182-024-03284-0.
10. Grenadyorov A.S., Chebodaeva V.V., Khlusov I.A., Semin V.O., Madzhara N.E., Solovyev A.A. Effect of a-C:H:SiOx coating thickness on corrosion resistance and zeta potential level of Ti-6Al-4V. *Journal of Vacuum Science & Technology A*. 2025;43(2):023401. DOI: 10.1116/6.0004085.
11. Evtushenko D.N., Fateev A.V., Khainovsky M.A., Polishchuk J., Kokorev O.V., Nasibov T.F. et al. Intermolecular interactions, regioselectivity, and biological activity of L-ascorbic acid, nicotinic acid and their cocrystal. *CrystEngComm*. 2024;26(46):6650–6666. DOI: 10.1039/d4ce00770k.
12. Nasibov T., Gorokhova A., Porokhova E., Shupletsova V., Yurova K., Avdeeva E. et al. A hypothesis of mesenchymal stem cell osteogenic differentiation mediated by chelidonic acid through the calcium import: original research and computer simulation. *Histochemistry and Cell Biology*. 2025;163(1):14. DOI: 10.1007/s00418-024-02342-5.
13. Nasibov T.F., Gorokhova A.V., Brazovsky K.S., Porokhova E.D., Avdeeva E.Yu., Belousov M.V. et al. The pipeline for in silico prediction of target genes and target metabolic pathways for small molecules, using chelidonic acid as an example. *Advanced targets in Biomedicine*. 2025;1(1):6–19. DOI: 10.5922/ATB-2025-1-1-1.
14. Korkmaz S., Goksuluk D., Zararsiz G. MVN: An R package for assessing multivariate normality. *The R Journal*. 2014;6(2):151–162.
15. PMCMRplus (version 1.9.12). Rdocumentation [Internet]. URL: https://www.rdocumentation.org/packages/PMCMRplus/versions/1.9.12.
16. brunnermunzel (version 2.0). Rdocumentation [Internet]. [cited 2024 Jul 21]. URL: https://www.rdocumentation.org/packages/brunnermunzel/versions/2.0
17. Royston P. Remark AS R94: A remark on algorithm AS 181: the W-test for normality. *Journal of the Royal Statistical Society. Series C (Applied Statistics)*. 1995;44(4):547–551. DOI: 10.2307/2986146.
18. Moser B.K., Stevens G.R. Homogeneity of variance in the two-sample means test. *The American Statistician*. 1992;46(1):19–21. DOI: 10.1080/00031305.1992.10475839.
19. Coombs W.T., Algina J., Oltman D.O. Univariate and multivariate omnibus hypothesis tests selected to control type I error rates when population variances are not necessarily equal. *Review of Educational Research*. 1996;66(2):137–179. DOI: 10.3102/00346543066002137.
20. Markowski C.A., Markowski E.P. Conditions for the effectiveness of a preliminary test of variance. *The American Statistician*. 1990;44(4):322–326. DOI: 10.1080/00031305.1990.10475752
21. Smith,H.F, The problem of comparing the results of two experiments with unequal errors. *Journal of the Council for Scientific and Industrial Research.* 1936;9:211–212.
22. Satterthwaite F.E. An approximate distribution of estimates of variance components. *Biometrics Bulletin*. 1946;2(6):110–114. DOI: 10.2307/3002019.
23. Welch B.L. The significance of the difference between two means when the population variances are unequal. *Biometrika*. 1938;29(3/4):350–362. DOI: 10.2307/2332010.
24. Moser B.K., Stevens G.R., Watts C.L. The two-sample *t* test versus Satterthwaite's approximate *F* test. *Communications in Statistics-Theory and Methods*. 1989;18(11):3963–3975. DOI: 10.1080/03610928908830135.
25. Zimmerman D.W., Zumbo B.D. Rank transformations and the power of the Student *t* test and Welch *t* test for non-normal populations with unequal variances. *Canadian Journal of Experimental Psychology / Revue canadienne de psychologie expérimentale*. 1993;47(3):523. DOI: 10.1037/h0078850.

26. Ruxton G.D. The unequal variance t-test is an underused alternative to Student's *t*-test and the Mann – Whitney *U*-test. *Behavioral Ecology*. 2006;17(4):688–690. DOI: 10.1093/beheco/ark016.
27. Munzel U., Brunner E. Nonparametric tests in the unbalanced multivariate one-way design. *Biometrical Journal*. 2000;42(7):837–854. DOI: 10.1002/1521-4036(200011)42:7<837::AID-BIMJ837>3.0.CO;2-S.
28. Brunner E., Munzel U. The nonparametric Behrens – Fisher problem: asymptotic theory and a small-sample approximation. *Biometrical Journal*. 2000;42(1):17–25. DOI: 10.1002/(SICI)1521-4036(200001)42:1<17::AID-BIMJ17>3.0.CO;2-U.
29. Karch J.D. Psychologists should use Brunner – Munzel's instead of Mann – Whitney's *U*- test as the default nonparametric procedure. *Advances in Methods and Practices in Psychological Science*. 2021;4(2): 2515245921999602. DOI: 10.1177/2515245921999602.
30. Noguchi K., Konietschke F., Marmolejo-Ramos F., Pauly M. Permutation tests are robust and powerful at 0.5% and 5% significance levels. *Behavior Research Methods*. 2021;53(6):2712–2724. DOI: 10.3758/s13428-021-01595-5.
31. Celik N. Welch's ANOVA: Heteroskedastic skew-t error terms. *Communications in Statistics-Theory and Methods*. 2022.;51(9):3065–3076. DOI: 10.1080/03610926.2020.1788084.
32. Delacre M., Lakens D., Leys C. Why psychologists should by default use Welch's *t*-test instead of Student's *t*-test. *International Review of Social Psychology*. 2017;30(1):92–101. DOI: 10.5334/irsp.82.
33. Tomarken A.J., Serlin R.C. Comparison of ANOVA alternatives under variance heterogeneity and specific noncentrality structures. *Psychological Bulletin*. 1986; 99(1):90. DOI: 10.1037/0033-2909.99.1.90.
34. Levy K.J. An empirical comparison of the ANOVA F-test with alternatives which are more robust against heterogeneity of variance. *Journal of Statistical Computation and Simulation*. 1978;8(1):49–57. DOI: 10.1080/00949657808810247.
35. Lix L.M., Keselman J.C., Keselman H.J. Consequences of assumption violations revisited: A quantitative review of alternatives to the one-way analysis of variance *F* test. *Review of Educational Research*. 1996;66(4):579–619. DOI: 10.3102/00346543066004579.
36. Tamhane A.C. A comparison of procedures for multiple comparisons of means with unequal variances. *Journal of the American Statistical Association*. 1979:74(366a):471–480. DOI: 10.1080/01621459.1979.10482541.
37. Shingala M.C., Rajyaguru A. Comparison of post hoc tests for unequal variance. *International Journal of New Technologies in Science and Engineering*. 2015;2(5):22–33.
38. Berridge M.V., Herst P.M., Tan A.S. Tetrazolium dyes as tools in cell biology: new insights into their cellular reduction. *Biotechnology Annual Review*. 2005;11:127–152. DOI: 10.1016/S1387-2656(05)11004-7.
39. Ghasemi M., Turnbull T., Sebastian S., Kempson I. The MTT Assay: Utility, Limitations, Pitfalls, and Interpretation in Bulk and Single-Cell Analysis. *International Journal of Molecular Sciences*. 2021;22(23):12827. DOI: 10.3390/ijms222312827.
40. Ren Q., Zhu X., Li W., Wu M., Cui S., Ling Y. et al. Fabrication of super-hydrophilic and highly open-porous poly (lactic acid) scaffolds using supercritical carbon dioxide foaming. *International Journal of Biological Macromolecules*. 2022;205:740–748. DOI: 10.1016/j.ijbiomac.2022.03.107.
41. Long J., Zhong M., Zhang H., Fan P. Superhydrophilicity to superhydrophobicity transition of picosecond laser microstructured aluminum in ambient air. *Journal of Colloid and Interface Science*. 2015;441:1–9. DOI: 10.1016/j.jcis.2014.11.015.
42. Razi S., Mollabashi M., Madanipour K. Improving the hydrophilicity of metallic surfaces by nanosecond pulsed laser surface modification. *Journal of Laser Applications*. 2015;27(4):042006-1–042006-9. DOI: 10.2351/1.4928290.
43. Zhu H.Z., Zhang H.C., Ni X.W., Shen Z.H., Lu J. Fabrication of superhydrophilic surface on metallic nickel by sub-nanosecond laser-induced ablation. *AIP Advances*. 2019;9(8):085308. DOI: 10.1063/1.5111069.
44. Ganash M.A. Anticancer potential of ascorbic acid and inorganic selenium on human breast cancer cell line MCF-7 and colon carcinoma HCT-116. *Journal of Cancer Research and Therapeutics*. 2021;17(1):122–129. DOI: 10.4103/jcrt.JCRT_989_17.
45. Mobasher M.A. Apoptotic activity and cytotoxic effect of convolvulus spicatus on human breast cancer cell line (MCF-7). *Pakistan Journal of Biological Sciences*. 2021;24(6):646–655. DOI: 10.3923/pjbs.2021.646.655.
46. Gambardella G., Viscido G., Tumaini B., Isacchi A., Bosotti R., di Bernardo D. A single-cell analysis of breast cancer cell lines to study tumour heterogeneity and drug response. *Nature Communications*. 2022;13(1):1714. DOI: 10.1038/s41467-022-29358-6.
47. Fayyad R.J., Ali A.N.M., Saeed N.A.A.A.H., Hamzah I.H., Dwaish A.S. Phycosynthesis of silver nanoparticles *using Cladophora glomerata* and evaluation of their ability to inhibit the proliferation of MCF-7 and L20B cell lines. *Asian Pacific Journal of Cancer Prevention: APJCP*. 2022;23(10):3563–3569. DOI: 10.31557/APJCP.2022.23.10.3563.
48. Komarova E.G., Akimova E.B., Kondranova A.M., Porokhova E.D., Nasibov T.F., Syrokvashin M.M. et al. Laser interference microscopy study of the morphometric features of MCF-7 cancer cells contacted with 5-Fluorouracil-loaded calcium phosphate coatings on titanium implants. *Materials Chemistry and Physics*. 2025;333:130299. DOI: 10.1016/j.matchemphys.2024.130299.
49. Zohrabi T., Habibi N., Zarrabi A., Fanaei M., Lee L.Y. Diphenylalanine peptide nanotubes self-assembled on functionalized metal surfaces for potential application in drug-eluting stent. *Journal of Biomedical Materials Research. Part A*. 2016;104(9):2280–2290. DOI: 10.1002/jbm.a.35764.
50. Pintor A.V.B., Queiroz L.D., Barcelos R., Primo L.S.G., Maia L.C., Alves G.G. MTT versus other cell viability assays to evaluate the biocompatibility of root canal filling materials: a systematic review. *International Endodontic Journal*. 2020;53(10):1348–1373. DOI: 10.1111/iej.13353.
51. Ohashi K., Fujiwara S., Mizuno K. Roles of the cytoskeleton, cell adhesion and rho signalling in mechanosensing and mechanotransduction. *The Journal of Biochemistry*. 2017;161(3):245–254. DOI: 10.1093/jb/mvw082.
52. Burridge K., Monaghan-Benson E., Graham D.M. Mechanotransduction: from the cell surface to the nucleus via

RhoA. *Philosophical Transactions of the Royal Society B*. 2019;374(1779):20180229. DOI: 10.1098/rstb.2018.0229.
53. Janota C.S., Calero-Cuenca F.J., Gomes E.R. The role of the cell nucleus in mechanotransduction. *Current Opinion in Cell Biology*. 2020;63:204–211. DOI: 10.1016/j.ceb.2020.03.001.
54. Khlusov I.A., Litvinova L.S., Yurova K.A., Khlusova M.Y. Precise tissue bioengineering and niches of mesenchymal stem cells: their size and hierarchy matter. *Biocell*. 2022;46(6):1365–1373. DOI: 10.32604/biocell.2022.018917.
55. Khlusov I.A., Khlusova M.Yu., Litvinova L.S. Native cell domains as stem cell regulatory microterritories for precise tissue engineering. *Next Materials*. 2023;1(3):100021. DOI: 10.1016/j.nxmate.2023.100021.
56. Spriano S., Sarath Chandra V., Cochis A., Uberti F., Rimondini L., Bertone E. How do wettability, zeta potential and hydroxylation degree affect the biological response of biomaterials? *Materials Science and Engineering: C*. 2017;74:542–555. DOI: 10.1016/j.msec.2016.12.107.
57. Song J., Gerecht S. Hydrogels to recapture extracellular matrix cues that regulate vascularization. *Arteriosclerosis, Thrombosis, and Vascular Biology*. 2023;43(8):e291–e302. DOI: 10.1161/ATVBAHA.122.318235.
58. Khlusov I.A., Grenadyorov A.S., Solovyev A.A., Semenov V.A., Zhulkov M.O., Sirota D.A. et al. Endothelial cell behavior and nitric oxide production on a-C:H:SiOx-coated Ti-6Al-4V substrate. *International Journal of Molecular Sciences*. 2023;24(7):6675. DOI: 10.3390/ijms24076675.
59. Zhang M., Zhao F., Zhu Y., Brouwer L.A., Van der Veen H., Burgess J.K. et al. Physical properties and biochemical composition of extracellular matrix-derived hydrogels dictate vascularization potential in an organ-dependent fashion. *ACS Applied Materials & Interfaces*. 2024;16(23):29930–29945. DOI: 10.1021/acsami.4c05864.
60. Grenadyorov A.S., Solovyev A.A., Oskomov K.V., Semenov V.A., Zhulkov M.O., Sirota D.A. et al. Morphofunctional reaction of leukocytes and platelets in in vitro contact with a-C:H:SiOx-coated Ti-6Al-4V substrate. *Journal of Biomedical Materials Research. Part A*. 2023;111(3):309–321. DOI: 10.1002/jbm.a.37470.
61. Belosludtsev K.N., Belosludtseva N.V., Agafonov A.V., Penkov N.V., Samartsev V.N., Lemasters J.J. et al. Effect of surface-potential modulators on the opening of lipid pores in liposomal and mitochondrial inner membranes induced by palmitate and calcium ions. *Biochimica et Biophysica Acta (BBA) – Biomembranes*. 2015;1848(10):2200–2205. DOI: 10.1016/j.bbamem.2015.05.013.
62. Oberleithner H. Quantifying salt sensitivity. *Biological Chemistry*. 2021;402(12):1597–1602. DOI: 10.1515/hsz-2021-0206.
63. Ghitescu L., Fixman A. Surface charge distribution on the endothelial cell of liver sinusoids. *The Journal of Cell Biology*. 1984;99(2):639–647. DOI: 10.1083/jcb.99.2.639.
64. Lee K.S., Lee J., Kim H.K., Yeom S.H., Woo C.H., Jung Y.J. et al. Extracellular vesicles from adipose tissue-derived stem cells alleviate osteoporosis through osteoprotegerin and miR-21-5p. *Journal of Extracellular Vesicles*. 2021;10(12):e12152. DOI: 10.1002/jev2.12152.
65. Ouyang L., Shaik R., Xu R., Zhang G., Zhe J. Mapping surface charge distribution of single-cell via charged nanoparticle. *Cells*. 2021;10(6):1519. DOI: 10.3390/cells10061519.
66. Mao A.W., Jiang T.H., Sun X.J., Peng J. Application of chemokine receptor antagonist with stents reduces local inflammation and suppresses cancer growth. *Tumor Biology*. 2015;36(11):8637–8643. DOI: 10.1007/s13277-015-3557-1.
67. Venault A., Hsu K.J., Yeh L.C., Chinnathambi A., Ho H.T., Chang Y. Surface charge-bias impact of amine-contained pseudozwitterionic biointerfaces on the human blood compatibility. *Colloids and Surfaces B: Biointerfaces*. 2017;151:372–383. DOI: 10.1016/j.colsurfb.2016.12.040.
68. Choi S.Y., Habimana O., Flood P., Reynaud E.G., Rodriguez B.J., Zhang N. et al. Material- and feature-dependent effects on cell adhesion to micro injection moulded medical polymers. *Colloids and Surfaces B: Biointerfaces*. 2016;145:46–54. DOI: 10.1016/j.colsurfb.2016.04.032.
69. Mirzadeh H., Moghadam E.V., Mivehchi H. Laser-modified nanostructures of PET films and cell behavior. *Journal of Biomedical Materials Research. Part A*. 2011;98(1):63–71. DOI: 10.1002/jbm.a.33097.
70. Anderson C.R., Gambinossi F., DiLillo K.M., Laschewsky A., Wischerhoff E., Ferri J.K. et al. Tuning reversible cell adhesion to methacrylate-based thermoresponsive polymers: effects of composition on substrate hydrophobicity and cellular responses. *Journal of Biomedical Materials Research Part A*. 2017;105(9):2416–2428. DOI: 10.1002/jbm.a.36100.
71. Lamichhane S., Anderson J.A., Remund T., Sun H., Larson M.K., Kelly P. et al. Responses of endothelial cells, smooth muscle cells, and platelets dependent on the surface topography of polytetrafluoroethylene. *Journal of Biomedical Materials Research. Part A*. 2016;104(9):2291–304. DOI: 10.1002/jbm.a.35763.
72. Tan L., Xie Q., Jia X., Guo M., Zhang Y., Tang H. et al. Dynamic measurement of the surface stress induced by the attachment and growth of cells on Au electrode with a quartz crystal microbalance. *Biosensors and Bioelectronics*. 2009;24(6):1603–1609. DOI: 10.1016/j.bios.2008.08.021.
73. Xie Y., Sproule T., Li Y., Powell H., Lannutti J.J., Kniss D.A. Nanoscale modifications of PET polymer surfaces via oxygen-plasma discharge yield minimal changes in attachment and growth of mammalian epithelial and mesenchymal cells in vitro. *Journal of Biomedical Materials Research: An Official Journal of The Society for Biomaterials, The Japanese Society for Biomaterials, and The Australian Society for Biomaterials and the Korean Society for Biomaterials*. 2002;61(2):234–245. DOI: 10.1002/jbm.10141.
74. Khorsandi L., Orazizadeh M., Niazvand F., Abbaspour M.R., Mansouri E., Khodadadi A. Quercetin induces apoptosis and necroptosis in MCF-7 breast cancer cells. *Bratislavske Lekarske Listy*. 2017;118(2):123–128. DOI: 10.4149/BLL_2017_025.
75. Zhu T., Wu J., Zhao N., Cai C., Qian Z., Si F. et al. Superhydrophobic / superhydrophilic Janus fabrics reducing blood loss. *Advanced Healthcare Materials*. 2018;7(7):e1701086. DOI: 10.1002/adhm.201701086.
76. Wu X.H., Liew Y.K., Mai C.W., Then Y.Y. Potential of superhydrophobic surface for bood-contacting medical devices. *International Journal of Molecular Sciences*. 2021;22(7):3341. DOI: 10.3390/ijms22073341.

77. Li H., Wang Y., Wu X., Zhou L., Liu L., Fang Y. Blood pump surface roughness: hemocompatibility and machining optimization. *ASAIO Journal*. 2025;10.1097. DOI: 10.1097/MAT.0000000000002501.

Author Contribution

Kokorev O.V. – developing the model, conducting co-cultivation of cells with nitinol samples, performing the MTT test. Gorokhova A.V. – morphometric processing and interpretation of experimental data, drafting and editing the article. Nasibov T.F. – conducting bioinformatics and statistical analysis, interpretation and visualization of data. Khlusov I.A. – collection and analysis of literary sources, drafting and editing of the article, coordination of the research. Krivoshchekov S.V. – measurement of cell zeta potential. Chebodaeva V.V. – measurement of the zeta potential of the flat surface of nitinol samples. Brazovsky K.S. – development of the algorithm for in silico modeling of intracellular signaling and metabolic pathways. Khlusova M.Yu. – collection and analysis of literary sources on the biology of the tested cells, participation in article editing. Sablina T.Yu. – collection and analysis of literary sources, conducting research after laser surface modification, interpretation and visualization of experimental data, drafting of a section of the article, editing of the article. Kandaurova M.Yu. – collection and analysis of literary sources, performing UV laser treatment of experimental samples, conducting physical research after laser surface modification, interpretation and visualization of experimental data, drafting of a section of the article. Zyatikov I.A. – performing UV laser treatment of experimental samples, conducting research after laser surface modification, interpretation and visualization of experimental data. Panchenko Yu.N. – coordination of research on laser surface modification of experimental samples, drafting and editing of the article.

Author Information

Khlusov Igor A. – Dr. Sci. (Med.), Professor, Division of Morphology and General Pathology, Siberian State Medical University, Tomsk; Head of the Laboratory of Cellular and Microfluidic Technologies, Siberian State Medical University, Tomsk; Senior Researcher, IHCE SB RAS, Tomsk, khlusov63@mail.ru, https://orcid.org/0000-0003-3465-8452

Kokorev Oleg V. – Dr. Sci. (Med.), Professor, Division of Biochemistry and Molecular Biology with a Course in Clinical Laboratory Diagnostics, Siberian State Medical University, Tomsk, https://orcid.org/0000-0003-3690-0177

Gorokhova Anna V. – Research Assistant, Division of Morphology and General Pathology, Siberian State Medical University, Tomsk; Engineer, IHCE SB RAS, Tomsk, a.gorokhova3062@gmail.com, https://orcid.org/0000-0001-8401-7181

Nasibov Temur F. – Research Assistant, Division of Morphology and General Pathology, Siberian State Medical University, Tomsk; Engineer, IHCE SB RAS, Tomsk, temur.nsbv@gmail.com, https://orcid.org/0000-0002-8056-3967

Krivoshchekov Sergey V. – Cand. Sci. (Chemistry), Associate Professor, Division of Pharmaceutical Analysis, Siberian State Medical University, Tomsk, krivoshchekov.sv@ssmu.ru, https://orcid.org/0000-0001-5505-7141

Chebodaeva Valentina V. – Cand. Sci. (Engineering), Researcher, ISPMS SB RAS, Tomsk; Junior Researcher, IHCE SB RAS, Tomsk, vtina5@mail.ru, https://orcid.org/0000-0002-1980-3941

Brazovsky Konstantin S. – Dr. Sci. (Engineering), Professor, Division of Medical and Biological Cybernetics, Siberian State Medical University, Tomsk, brazovsky.ks@ssmu.ru, https://orcid.org/ 0000-0002-4779-9820

Khlusova Marina Yu. – Cand. Sci. (Med.), Associate Professor, Pathophysiology Division, Siberian State Medical University, Tomsk, hlusova.my@ssmu.ru, https://orcid.org/0000-0001-9583-5358

Sablina Tatyana Yu. – Cand. Sci. (Engineering), Researcher, Gas Lasers Laboratory, IHCE SB RAS, Tomsk, sty@lgl.hcei.tsc.ru, https://orcid.org/0000-0002-5941-5732

Kandaurova Marina Yu. – Cand. Sci. (Physics and Mathematics), Researcher, Gas Lasers Laboratory, IHCE SB RAS, Tomsk, panchenko.marina4@gmail.com, https://orcid.org/0000-0003-0236-2227

Zyatikov Ilya A. – Junior Researcher, Gas Lasers Laboratory, IHCE SB RAS, Tomsk, zyatikov@lgl.hcei.tsc.ru, https://orcid.org/0000-0003-3219-9299

Panchenko Yuri N. – Dr. Sci. (Physics and Mathematics), Chief Researcher, Head of the Gas Lasers Laboratory, IHCE SB RAS, Tomsk, yu.n.panchenko@mail.ru, https://orcid.org/0000-0001-8017-7268

(✉) **Khlusov Igor A.,** khlusov63@mail.ru

Received on September 05, 2025;
approved after peer review on September 19, 2025;
accepted on September 25, 2025